ChemComm

Accepted Manuscript

Volume 52 | Number 1 | 4 January 2016 | Pages 1–216

ChemComm

Chemical Communications
www.rsc.org/chemcomm

ISSN 1359-7345

ROYAL SOCIETY OF CHEMISTRY

COMMUNICATION
Marilyn M. Olmstead, Alan L. Balch, Josep M. Poblet, Luis Echegoyen et al.
Reactivity differences of Sc$_3$N@C$_{2n}$ ($2n$ = 68 and 80). Synthesis of the first methanofullerene derivatives of Sc$_3$N@C$_{68}$

175 YEARS

ROYAL SOCIETY OF CHEMISTRY

rsc.li/chemcomm

ChemComm

COMMUNICATION

Exploration of organic-inorganic hybrid perovskites for surface-enhanced infrared spectroscopy of small molecules

Jia Chen,[a] Zhi-Hong Mo,*[ab] Xiao Yang,[a] Hai-Ling Zhou,[a] Qin Gao[a]

The organic-inorganic hybrid perovskites allow the infrared absorption of small molecules to be efficiently enhanced. It is suggested that the quantum wells of perovskites enable their electrons to be excited by the light in the infrared region. The exploration has opened a new path for chemical sensing through infrared spectroscopy.

Infrared spectroscopy caused by molecular vibrations is extremely powerful for identifying the presence of specific structures, charge states, and orientations of organic molecules.[1,2] However, its applications have been usually restricted to large sample amounts because of the poor infrared absorption inherent to the vibrational polarization. In 1980, Hartstein et al.[3] first found that the infrared absorption of molecules on metal films can be enhanced by a factor of 20. This effect is called surface-enhanced infrared absorption (SEIRA). Meanwhile, the surface-enhanced Raman scattering (SERS) has dramatic enhancements achieving single molecule detection with metallic nano-islands and nanoparticles as the substrates.[4] The reason is that a tremendous electric field around the nanostructure is produced from the excitation of free electrons in the metal by the incident photons in the visible region, which is referred to as localized surface plasmon resonance (LSPR).[5-7]

A similar mechanism of the enhancement effect might be considered in SEIRA. However, the LSPR frequencies of metals are generally located in the visible range due to their high carrier concentrations, and has been ultimately extended to the near-IR range by the rational design of the nanostructures.[8-11] Thus, the excitation of plasmonic fields across the broad mid-IR region needed for SEIRA is very hard to be achieved on metallic substrates. As a consequence, scientists have to exploit alternative materials

with lower carrier concentrations such as the doped materials,[12,13] metallic nitrides[14] and graphene[15,16] to realize the mid-IR plasmonic resonances.[17,18] Recently, the organic-inorganic perovskites have spectacularly emerged as the next leading generation of semiconductor materials with superior electronic and optical functions. This promising class of materials enable the integration of useful organic and inorganic characteristics within a single complex molecule, providing unique properties such as the excellent light harvesting and the high carrier mobility.[19-21] Up to date, the hybrid perovskites have been applied for various optoelectronic devices including photovoltaic cells, light-emitting diodes and photo-detectors.[22-24] Interestedly, incorporation of metal nanoparticles into hybrid perovskites has been explored to improve the performance of perovskite solar cells.[25,26] And the electron transfer between metal nanomaterials and perovskites has also been demonstrated.[27]

Here, we have for the first time discovered that the organic-inorganic halide perovskites can significantly induce the SEIRA of adsorbed organic molecules. As a special attention focused on detection of explosives, four nitroaromatic compounds, including trinitrophenol (TNP), p-nitrophenol (PNP), dinitrotoluene (DNT), paranitrotoluene (PNT), were used to demonstrate the enhancement capability of the hybrid perovskites for infrared spectroscopy of small molecules. All of the IR spectra were measured via transmission modes under the same detection condition. It was certified that the $CH_3NH_3PbI_3$ perovskite films resulted in great enhancements of the IR absorption bands of surface-adsorbed nitroaromatic molecules.

[a] College of Chemistry and Chemical Engineering, Chongqing University, Shapingba, Chongqing 401331, China
E-mail: zhihmo@cqu.edu.cn
[b] National Key Laboratory for New Micro/Nano-Devices and System Technology, Chongqing University, Shapingba, Chongqing 400044, China.
† Electronic Supplementary Information (ESI) available: Experimental procedures and additional figures. See DOI: 10.1039/x0xx00000x

COMMUNICATION

The X-ray diffraction patterns and the scanning electron micro-scopic image of the as-prepared $CH_3NH_3PbI_3$ perovskite (Fig. S1 and S2, ESI†) indicated that the material was of the perovskite type with well crystallization. Compared to the bare perovskite, the use of PMMA as a cooperative additive for the perovskite growth could enhances the morphological control over the polycrystalline film and exhibit increased moisture stability.[28] Here, the $CH_3NH_3PbI_3$-PMMA films prepared by annealing the mixture of the precursors of the perovskite with PMMA were optimised for the content of PMMA according to the IR absorption of the perovskite with higher intensity and better reproducibility (Fig. S3, ESI†). In addition, the positions of the characteristic IR peaks assigned to $CH_3NH_3PbI_3$ were not changed by the fabrication process, implying unchange of the perovskite structure. It was also demonstrated that the existence of PMMA in the $CH_3NH_3PbI_3$ perovskite film supplied a good stability lasting for 15 days under a humid environment (75% humidity, Fig. S4, ESI†). Based on those results, the $CH_3NH_3PbI_3$-PMMA film was subsequent-ly fabricated by using a solution containing 0.2 mol/L precursors and 10 mg/mL PMMA.

The IR detection of nitroaromatic analytes was performed as follows. A toluene solution of the analyte was dropcast onto and spread over the whole surface of the perovskite film, which was wettable by the solvent. And then a fast-heating process was applied to evaporate the solvent in a few minutes, avoiding the aggregation of analyte molecules. After that, no changes in the characteristic IR signals of the films were observed, indicating no disturbance to the perovskite film by the operation. And the same processes were performed on the blank substrate to ensure that the amount of analyte is the same for the perovskite surface and the blank substrate.

Fig. 1a shows the infrared spectra of the TNP molecule on the blank substrate (without the hybrid perovskite films), and on the film substrates of the $CH_3NH_3PbI_3$ alone and the $CH_3NH_3PbI_3$-PMMA
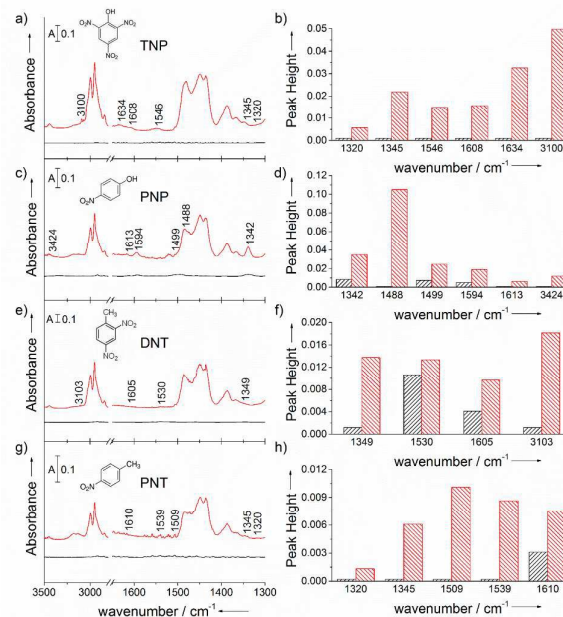
Fig. 2 IR detection of nitroaromatic molecules with a lower amount (0.25 $nmol/mm^2$). IR spectra (left) and peak heights of characteristic modes (right) of TNP (a,b), PNP (c,d), DNT (e,f) and PNT (g,h) on the blank substrate (black) and the perovskite-PMMA film (red), respectively.

composite, respectively. In order to avoid the interference of the infrared absorption of the perovskite and PMMA, we selected some characteristic peaks of the analytes for analysis which could be distinguished from the peaks of the substrate (marked in Fig.1a and 2a, also listed in Table S1, ESI†). Compared to the weak infrared absorptions of the TNP molecules on the blank substrate, it was clear to see that both the $CH_3NH_3PbI_3$ film and the $CH_3NH_3PbI_3$-PMMA film significantly enhanced the infrared signals of the TNP molecules. Hence, the $CH_3NH_3PbI_3$ perovskite was believed to function as an amplifier in infrared spectroscopy of small molecules. To most characteristic vibrational modes of the TNP molecule, the enhancement capability of the $CH_3NH_3PbI_3$-PMMA film was a little larger than that of the $CH_3NH_3PbI_3$ film, which indicated the existence of PMMA in the film would not reduce the surface enhancement. It might be contributed from the polymeric structure of PMMA, which would not hinder the contact of the analyte with the perovskite. The peak height of the infrared absorption, defined as the variation between the peak top and the lower adjacent bottom, was measured to show the enhancing effect more clearly. As shown in Fig. 1b, the results further proved that the two substrates with the $CH_3NH_3PbI_3$ film and the $CH_3NH_3PbI_3$-PMMA film, respectively, assisted in much higher absorption peaks than the blank substrate. The enhancement of absorption was from several times up to hundreds of times (for 3100 cm^{-1}). It should be noticed that the signal peaks at different wavenumbers were enhanced with different extents. It might be arisen from the orientation of the molecules adsorbed on the perovskite surface
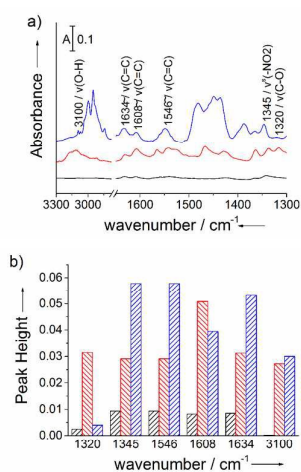

Fig. 1 SEIRA of TNP (2.5 $nmol/mm^2$) on the hybrid perovskite. a) IR spectra and b) peak heights of characteristic modes on the blank substrate (black), the perovskite film (red) and the perovskite-PMMA film (blue), respectively.

Please do not adjust margins
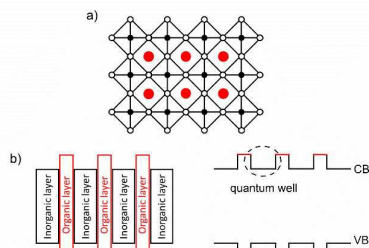
ChemComm

Journal Name

COMMUNICATION

Fig. 3 Analysis of the energy-levels of the hybrid perovskite. a) Schematic representation of layered perovskites. b) The quantum wells resulted from the alternative arrangement of the inorganic sheets and the organic layers of the hybrid perovskite.

(also see below), making different functional groups have different directions toward the surface and different distances from the surface.

The infrared spectra of a less amount of the four nitroaromatic analytes (0.25 nmol/mm^2) on the blank and the $CH_3NH_3PbI_3$-PMMA film substrates, respectively, were shown in Fig. 2. On the blank sub-strate, the IR signals of the analyte were too weak to be observed. However, the signals of all four molecules were obviously presented on the film substrate, indicating the nearly infinite enhancement of infrared absorption. The amount of the nitroaromatic analyte really contributed to the optical absorption was probably less than 1.1 nmol, which is estimated from the areal density of the TNP molecule and the spot area of the light beam (4.5 mm^2). It means that the IR detection limit of small molecules using the new SEIRA substrate could be greatly lowered down. Subsequently, more quantitative analyses were performed, and it was shown that the infrared absor-bance exhibited a good linear relationship with the areal density of the analyte (Fig. S6 and Table S2, ESI†). And thereof the lower limit of detection (LOD) was estimated to be less than 0.16 nmol/mm^2. In addition, the maximum relative standard deviation of the SEIRA detection of nitroaromatic molecules was about 4.5 % (for five repeats, 0.25 nmol/mm^2), demonstrating a good reproducibility of the assay. It was worth mentioned that the SEIRA substrate we used was of a non-optimized prototype, and great improvements can be achieved after further optimization such as the composition and morphology of hybrid perovskites, as well as the use of the analyte concentrating effect due to the wettability of various substrates.[29]

According to the surface selection rule, the vibrational modes that have dipole moment derivative components perpendicular to the surface are preferentially enhanced.[30,31] The orientation of the four nitroaromatic molecules adsorbed on the perovskite film has been analyzed by the infrared spectroscopy. The peaks around 1063 cm^{-1} attributed to vibrations of C-H in-plane and bending from the benzene ring are enhanced more than other vibrational modes (Fig. 1 for TNP and Fig. S5 for PNP, DNT and PNT, ESI†). It could be drawn that the nitroaromatic molecules were almost flat-lying on the surface. In addition, there were changes in IR peak positions corresponding to stretching vibrations of the aromatic C-H and the

nitro groups (Fig. S7, ESI†). It indicated that there existed not just the physical adsorption to the surface but also the chemical
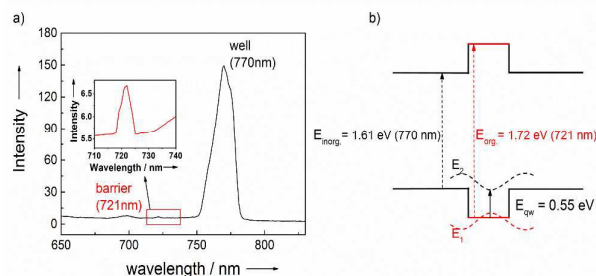

Fig. 4 Analysis of the electron transitions of the hybrid perovskite. a) Photo-luminescence spectrum of the perovskite (λ_{ex} = 330 nm). b) Schematic illustration of the energies of bandgaps and the electron transitions of the perovskite.

interaction of the small molecules with the $CH_3NH_3PbI_3$ perovskite, which was also been suggested in a previous report.[32]

The mechanism of the SEIRA using the $CH_3NH_3PbI_3$ perovskite was also analysed through the energy levels of the organic–inorganic perovskite. The basic layered perovskite structure is schematically depicted in Fig. 3a. Each of the inorganic sheets consists of corner-sharing metal halide octahedrons. Fig. 3b shows that the common arrangement of the energy bands in the material, where the conduction band (CB) of the inorganic sheets is substantially below that of the organic layers, and the valence band (VB) of the inorganic sheets is rationally above that of the organic layers. Therefore, the alternation of the inorganic sheets and the organic layers generate the quantum wells for both electrons and holes, resulting in very narrow bandgaps. Consequently, the electrons could be excited by the photons at longer wavelengths from the ground state of the quantum well (organic VB or inorganic CB) to the excited state (inorganic VB or organic CB). To prove this, photoluminescence (PL) measurements were performed, as shown in Fig. 4a. The PL peak at the longer wavelength of 770 nm in the $CH_3NH_3PbI_3$ was attributed to the electron transition from the VB maximum to the CB minimum of the inorganic sheets with a lower energy ($E_{inorg.}$ = 1.61 eV). The peak located at 721 nm corresponds mainly to a direct transition between the organic layers, giving a higher bandgap energy ($E_{org.}$ = 1.72 eV). According to Equation (1), the bandgap energy of the quantum well (E_{qw}) was less than 0.055eV calculated on the basis of the PL spectra.

$$E_{qw} \leq \frac{E_{org}-E_{inorg}}{2} = 0.055 \text{ eV} \qquad (1)$$

It meant that electrons of $CH_3NH_3PbI_3$ can be excited by photons in the mid-IR region (provide energy from 0.05 eV to 0.50 eV, see Fig. 4b), generating electron-hole pairs. The charge separation occurred in the hybrid perovskite was expected to induce electromagnetic changes and efficiently increase the dipolar polarization of the small molecules adjacent to the perovskite, which might be contributed to the enhancement of the infrared

Please do not adjust margins

COMMUNICATION

Journal Name

absorption of molecular vibrations. Some properties of the perovskite material, such as the lower carrier recombination rate and the higher carrier mobility, enable the electron-hole pairs to have a longer diffusion distance and a longer lifetime, which benefits the surface enhancement of infrared absorption.

In conclusion, we demonstrated for the first time that the organic-inorganic perovskite films enable the acquisition of SEIRA spectra of small molecules. The new semiconducting substrate greatly enhanced most of the infrared absorptions of molecular vibrations, organic molecules, allowing the much more sensitive detection of small molecules with infrared spectroscopy. This enhancement effect was probably attributed to the electromagnetic coupling originated from the electron transitions across the much narrower bandgap of the quantum wells in the hybrid perovskite, which could be excited by the mid-IR light. To go a step further, more efforts would be made to deeply unravel the complex mechanisms involved in the surface-enhanced spectroscopic process using the organic-inorganic perovskite films. Besides, additional polymers pro-tecting the perovskite film while giving minimal infrared absorption peaks, such as the simplest polymer polyethylene, could be explored to create a background as clean as possible, such that the spectral window for analyte detection is clear and unambiguous. Our exploration of the hybrid perovskites not only opens up a new direction for the search the holy grail of SEIRA similar to SERS, but also help to build one big new brick of the promising applications of the superior material.

Acknowledgements

Notes and references

1   B. Stuart, Infrared Spectroscopy, Kirk-Othmer Encyclopedia of Chemical Technology, 2005.
2   M. López-López and C. García-Ruiz, *Tr. Anal. Chem.*, 2014, **54**, 36–44.
3   A. Hartstein, J. R. Kirtley and J. C. Tsang, *Phys. Rev. Lett.,* 1980, **45**, 201-204.
4   K. Kneipp, Y. Wang, H. Kneipp, L. T. Perelman, I. Itzkan, R. R. Dasari and M. S. Feld, *Phys. Rev. Lett.,* 1997, **78**, 1667.
5   Z. Y. Li and Y. Xia, *Nano Lett.,* 2010, **10**, 243-249.
6   S. Zeng, D. Baillargeat, H. P. Ho and K. T. Yong, *Chem. Soc. Rev.*, 2014, **43**, 3426-3452.
7   S. Schlücker, *Angew. Chem. Int. Ed.*, 2014, **53**, 4756–4795.
8   M. Navarro-Cia and S. A. Maier, ACS Nano, 2012, 6, 3537–3544.
9   H. Chen, A. M. Bhuiya, R. Liu, D. M. Wasserman and K. C. Toussaint, Jr., *J. Phys. Chem. C,* 2014, **118**, 20553−20558.
10 L. Zhang, K. Xia, Z. Lu, G. Li, J. Chen, Y. Deng, S. Li, F. Zhou and N. He, *Chem. Mater.,* 2014, **26**, 1794−1798.
11 L. Lin and Y. Zheng, Sci. Rep., 2015, 5, 14788.
12 L. W. Chou, N. Shin, S. V. Sivaram and M. A. Filler, *J. Am. Chem. Soc.,* 2012, **134**, 16155−16158.
13 D. J. Rowe, J. S. Jeong, K. A. Mkhoyan and U. R. Kortshagen, *Nano Lett.,* 2013, **13**, 1317−1322.
14 P. K. Palomaki, E. M. Miller and N. R. Neale, *J. Am. Chem. Soc.,* 2013, **135**, 14142-14150.
15 M. Jablan, H. Buljan and M. Soljacic, *Phys. Rev. B,* 2009, **80**, 308-310.
16 D. Rodrigo, O. Limaj, D. Janner, D. Etezadi, F. J. G. De Abajo, V. Pruneri, V. Pruneri and H. Altug, *Science,* 2015, **349**, 165-168.
17 R. Stanley, *Nat. Photon.,* 2012, **6**, 409–411.
18 G. V. Naik, V. M. Shalaev and A. Boltasseva, *Adv. Mater.,* 2013, **25**, 3264-3294.
19 X. Zhu, *Acc. Chem. Res.,* 2016, **49**, 355-356.
20 B. Saparov and D. B. Mitzi, *Chem. Rev.*, 2016, **116**, 4558–4596.
21 T. M. Brenner, D. A. Egger, L. Kronik, G. Hodes and D. Cahen, *Nat. Rev. Mater.,* 2016, **1**, 15007.
22 S. Kazim, M. K. Nazeeruddin, M. Graetzel and S. Ahmad, *Angew. Chem. Int. Ed.,* 2014, **53**, 2812-2824.
23 S. D. Stranks and H. J. Snaith, *Nat. Nanotechnol.*, 2015, **10**, 391–402.
24 C. C. Stoumpos and M. G. Kanatzidis, *Adv. Mater.,* 2016, **28**, 5778–5793.
25 W. Zhang, M. Saliba, S. D. Stranks, Y. Sun, X. Shi, U. Wiesner and H.J. Snaith, *Nano Lett.,* 2013, **13**, 4505-4510.
26 S. Carreteropalacios, M. E. Calvo and H. Míguez, *J. Phys. Chem. C,* 2015, **119**, 18635-18640.
27 D. Xu, D. Liu, T. Xie, Y. Cao, J.-G. Wang, Z.-J. Ning, Y.-T. Long and H. Tian, *Chem. Commun.,* 2016, **52**, 9933-9936.
28 S. Masi, A. Rizzo, F. Aiello, F. Balzano, G. Uccellobarretta, A. Listorti, G. Gigliac and S. Colella, *Nanoscale,* 2015, **7**, 18956-18963.
29 F. De Angelis, F. Gentile, F. Mecarini, G. Das, M. Moretti, P. Candeloro, M. L. Coluccio, G. Cojoc, A. Accardo, C. Liberale, R. P. Zaccaria, G. Perozziello, L. Tirinato, A. Toma, G. Cuda, R. Cingolani, E. Di Fabrizio, *Nat. Photon.*, 2011, **5**, 682–687.
30 M. Osawa, K. I. Ataka, K. Yoshii and Y. Nishikawa, *Appl. Spectrosc.*, 1993, **47**, 1497-1502.
31 E. Pazos, A. M. Garcia, C. Penas, M. Nazarenus, A. Torruella, N. Pazos-Perez, L. Guerrini, M. E. Vázquez, E, Garcia-Rico, J. L. Mascareñas and R. A. Alvarez-Puebla, *J. Am. Chem. Soc.,* 2016, **138**, 14206–14209.
32 C. Muthu, S. Nagamma and V. Nair, *RSC Adv.* 2014, **4**, 55908-55911.